Coherent dynamics and terahertz emission in an asymmetric quantum well coupled to broadband infrared pulses

2004 J. Phys.: Condens. Matter 16 3411

(http://iopscience.iop.org/0953-8984/16/20/012)

INSTITUTE OF PHYSICS PUBLISHING JOURNAL OF PHYSICS: CONDENSED MATTER

J. Phys.: Condens. Matter **16** (2004) 3411–3420 PII: S0953-8984(04)77516-5

Coherent dynamics and terahertz emission in an asymmetric quantum well coupled to broadband infrared pulses

B H Wu and J C Cao

State Key Laboratory of Functional Materials for Informatics, Shanghai Institute of Microsystem and Information Technology, Chinese Academy of Sciences, 865 Changning Road, Shanghai 200050, People's Republic of China

Received 10 March 2004
Published 7 May 2004
Online at stacks.iop.org/JPhysCM/16/3411
DOI: 10.1088/0953-8984/16/20/012

Abstract

A selected intersubband transition in the asymmetric quantum well is theoretically proposed by using the superposition of two identical time delayed and phase shifted broadband pulses. Three conduction subbands in the semiconductor quantum well structure are optically coupled with the ultrafast infrared pulses. By adjusting the delay between these two pulses, the carriers at ground level can be selectively pumped to one of the upper levels, while the other upper level remains unoccupied. Thus selective transitions in the three level model can be manipulated by optical interference. At the same time, terahertz radiation will be emitted by coherent controlled charge oscillations. The phase and amplitude of THz radiation is found to be sensitive to the optical interference of the coupling pulses.

1. Introduction

Interaction between multilevel systems and the multifrequency laser fields have been associated with many complex nonlinear behaviours [1–7]. Investigations of the nonequilibrium dynamics of elementary excitations in bulk and nanostructured semiconductors via femtosecond infrared spectroscopy have been reviewed by Elsaesser *et al* [5]. Schemes for lasing without inversion, state trapping and selective transition in the atomic systems have been proposed based on the quantum coherence between atomic levels [4, 8, 9]. In semiconductors, the dephasing time for coherent carriers, with a typical value below 1 ps, is much shorter than that of the atoms or molecules. Due to the application of femtosecond lasers, optically induced coherent carrier phenomena in semiconductor nanostructures, such as the coherent control and enhancement of the refractive index in an asymmetric double quantum well, charge oscillations in a double quantum well, and Bloch oscillations in superlattices have been proposed and observed [10–18]. Coherence control implies that not only the amplitude but also the phase conditions

become important for the characteristics of the systems. The coherent control of excitons in a quantum well with a pair of phase locked ultrashort pulses was displayed by Heberle *et al* [19, 20]. The intersubband transition in semiconductor nanostructures has played an important role in mid-to far-infrared optoelectronic devices, such as the quantum well infrared photodetector and quantum cascade lasers [21]. Efforts have been made to realize mid-to far-infrared emission from an optically pumped infrared intersubband laser [22, 23]. Methods to control the subband population have an important meaning for these applications. A key challenge and prerequisite in the design of a laser based on intersubband transitions is to obtain population inversion. If we want mid-to far-infrared light to be generated from semiconductor nanostructures by optical pumping, we must have a population inversion between the two lasing subbands. Electrons in the ground subband must be selectively pumped to the upper lasing level by the ultrafast pumping pulse. This selective pumping can be accomplished with a spectrally narrow tunable excitation source. But when the optical pumping pulse is ultrafast, or in other words, spectrally wide, this is not easy, especially when the upper two subbands have a very small energy difference. An ultrafast optical pulse cannot distinguish them when pumping electrons from the ground state. Electrons can be pumped to either of the upper subbands simultaneously. In the following, a scheme for coherent control of any selective subband population filling by optical injection is presented. Any desired subband population can be realized by carefully adjusting the parameters through this scheme.

2. Theoretical model

In this paper, we demonstrate our proposal for overcoming the problem of selective *intersubband* transition in an asymmetric quantum well structure based on the interference of light, using a superposition of two identical, time delayed and phase shifted optical pulses. As an example, we consider an asymmetric quantum well, as shown in figure 1. Only the lowest three conduction subbands are taken into account in our calculation. Carriers in the ground level can transit to the upper electron subbands, subband 2 or subband 3, by absorbing a photon. If a laser has a short pulsewidth, the corresponding spectral width will expand. For example, the pulsewidth of a 1 ps laser pulse has at least 15 cm^{-1} spectral width. These spectral components of the pulse can interact with the nonlinear optical system. Thus, when an ultrafast pulse (also a broadband pulse from the spectrum's point of view) is imposed on this system, the electrons in the ground level can be pumped to either of the upper subbands according to their spectrum intensity. If we carefully adjust the time delay and phase shift of the two identical ultrafast pulses, we can bring one of the intersubband transitions into the 'hole' of the interference pattern and keep it unexcited. The double intersubband transitions can be selectively controlled on the femtosecond timescale.

We consider a superposition of two identical time delayed and phase shifted ultrafast pulses. The total light field has the form

$$\begin{aligned} E_\Sigma(t) = E_1(t) + E_2(t) = {} & \tfrac{1}{2}A_0(t)\exp[\mathrm{i}\omega_0 t] + \tfrac{1}{2}A_0(t)\exp[-\mathrm{i}\omega_0 t] \\ & + \tfrac{1}{2}A_0(t-\Delta\tau)\exp[\mathrm{i}\omega_0(t-\Delta\tau) + \mathrm{i}\Delta\psi] \\ & + \tfrac{1}{2}A_0(t-\Delta\tau)\exp[-\mathrm{i}\omega_0(t-\Delta\tau) - \mathrm{i}\Delta\psi], \end{aligned} \tag{1}$$

where $E_\Sigma(t)$ is the total light field, $A_0(t)$ is the amplitude of the ultrafast pulse, ω_0 is the frequency of the pulse, and $\Delta\tau$ is the time delay, and $\Delta\psi$ the phase shift, of the two pulses. In our case, $A_0(t)$ has a Gaussian envelope for simplicity.

In order to get the spectrum, we have to rely on its Fourier transform. Here the Fourier transform properties of time delay and frequency shifting are needed. After performing a

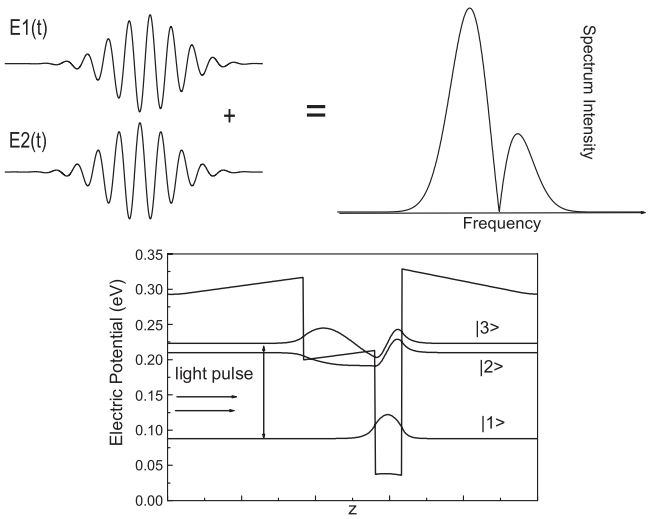

Figure 1. The superposition of two identical time delayed and phase shifted ultrashort pulses, the potential profile of the nanostructure and the lowest three subband wavefunctions of the asymmetric quantum well structure. Selective transitions are induced by the interference of these two pulses. There are holes in the spectrum after the interference. If one of the transitions is placed in the hole, the excitation will be suppressed.

Fourier transform we can get the spectrum function as

$$\begin{aligned} F_\Sigma(\omega) &= \tfrac{1}{2}F_0(\omega+\omega_0) + \tfrac{1}{2}F_0(\omega-\omega_0) + \tfrac{1}{2}F_0(\omega+\omega_0)\mathrm{e}^{\mathrm{i}\omega\Delta\tau+\mathrm{i}\Delta\psi} + \tfrac{1}{2}F_0(\omega-\omega_0)\mathrm{e}^{\mathrm{i}\omega\Delta\tau-\mathrm{i}\Delta\psi} \\ &= F_0(\omega+\omega_0)\cos((\omega\Delta t+\Delta\psi)/2)\mathrm{e}^{\mathrm{i}(\omega\Delta\tau+\Delta\psi)/2} \\ &\quad + F_0(\omega-\omega_0)\cos((\omega\Delta\tau-\Delta\psi)/2)\mathrm{e}^{\mathrm{i}(\omega\Delta\tau-\Delta\psi)/2}, \end{aligned} \tag{2}$$

where $F_0(\omega)$ is the Fourier spectrum of the amplitude of the ultrafast pulse $A_0(t)$ and $F_\Sigma(\omega)$ is the Fourier spectrum of the total light field. Equation (2) is the general relation of $F_\Sigma(\omega)$.

Only the spectrum part where the frequency is around ω_0 plays an important role in the pumping of electrons. The resulting spectrum is

$$|F_\Sigma(\omega)| \simeq |F_0(\omega-\omega_0)|\cos((\omega\Delta\tau-\Delta\psi)/2). \tag{3}$$

Thus the spectrum of the combined field will be sinusoidally modulated by the optical interference. When the phase of the modulation satisfies

$$\omega\Delta\tau - \Delta\psi = \pi(2k+1), \tag{4}$$

where $k = 0, \pm1, \ldots$ is any integer, the intensity of the spectral components at frequency $\omega_k = [\pi(2k+1) + \Delta\psi]/\Delta\tau$ equals zero. This interference is schematically depicted in figure 1 to give a physical picture. The interval between the two zero spectrum intensity frequencies can be adjusted by the time delay $\Delta\tau$, while the variation of the phase shift $\Delta\psi$ translates the whole interference structure along the frequency axis.

When an ultrafast pulse possesses a large bandwidth and the energy split of the upper two subbands is small enough, it is possible that both the intersubband transitions from the ground subband to subband 2 and subband 3 will be coupled to this pulse. If we choose the frequency to be one of the double intersubband transitions belonging to the zero spectrum intensity frequencies by varying the phase conditions, then this particular transition will be suppressed. In other words, the carriers in the ground level will not be allowed to be pumped to this subband. At the same time, the other intersubband transition can be achieved if the frequency does not fall into the 'holes' in the interference spectrum. Thus a selective transition can be achieved. For example, if the time delay is fixed and the phase shift condition is set to be $\Delta\psi = \pi + \omega_{21}\Delta\tau$, the transition from the ground subband to subband 2 will be suppressed. This selectivity is valid for the transition between subband 1 and subband 3 by replacing ω_{21} by ω_{31} in the preceding relation.

The microscopic analysis of coherent effects in photoexcited semiconductors is based on the semiconductor Bloch equations within the three subband model [24–26]. In the second quantization, the Hamiltonian of this system in the absence of any infrared fields can be written as

$$H = H_0 + H_{\mathrm{Coul}} = \sum_{\mu} \varepsilon_{\mu,k} a^{\dagger}_{\mu,k} a_{\mu,k} + \tfrac{1}{2} \sum_{\mu\nu\mu'\nu'kk'q} V_q^{\mu\nu\nu'\mu'} a^{\dagger}_{\mu,k+q} a^{\dagger}_{\nu,k'-q} a_{\nu',k'} a_{\mu,k}, \tag{5}$$

where H_0 is the kinetic term, H_{Coul} represents the Coulomb interaction, ε_μ is the electron energy, and $a^{\dagger}_{\mu,k}$, $a_{\mu,k}$ are the electron creation and electron annihilation operator of the μth subband with a wavevector k [24, 25, 27]. $V_k^{\mu\mu'\nu\nu'}$ is the Coulomb matrix element. Under the dipole approximation, the light material interaction Hamiltonian has the form

$$\begin{aligned} H_{\mathrm{I}} = -\sum_{\mu,\mu',k} E(t)(d_{\mu,\mu',k} a^{\dagger}_{\mu,k} a_{\mu',k} + \mathrm{h.c.}) = -\sum_{\mu,\mu',k} (A_0(t)\cos(\omega_0 t) \\ + A_0(t-\Delta\tau)\cos(\omega_0(t-\Delta\tau)+\Delta\psi))(d_{\mu,\mu',k} a^{\dagger}_{\mu,k} a_{\mu',k} + \mathrm{h.c.}) \end{aligned} \tag{6}$$

where $d_{\mu,\mu',k}$ is the optical dipole matrix element. Since the splittings of the subbands are small (tens of meV), we have avoided the rotating wave approximation in the interaction Hamiltonian [11, 28, 29]. The electron–electron Coulomb interaction is treated within the screened Hartree–Fock approximation. The set of equations of motion for the electrons in the multisubband system can be directly deduced from Heisenberg's equation of motion with a Hamiltonian including many-body effects and Coulomb interaction [24, 25]. The other various scattering and dephasing mechanisms, such as electron–phonon scattering or scattering by impurities, will be taken into account by introducing phenomenological decay and dephasing constants for simplicity [24, 25].

The quantities of interest are the electron distribution $n_{\mu,k}$, and the intersubband polarization $p_{\mu\nu,k}$. These can be defined as

$$n_{\mu,k} = \langle a^{\dagger}_{\mu,k} a_{\mu,k} \rangle \tag{7}$$

$$p_{\mu\nu,k} = \langle a^{\dagger}_{\nu,k} a_{\mu,k} \rangle, \tag{8}$$

where $\langle F \rangle$ is the expectation value of operator F. The expectation value $n_{\mu,k}$ is simply the population of the electrons at wavevector k in the μth subband, and $p_{\mu\nu,k}$ is related to the polarization of the medium, which becomes macroscopic because of the applied external field.

Based on these definitions and the Hamiltonian given above, we can derive the equation of motion for electron distribution and intersubband polarization [24, 25]. The starting point is the Heisenberg equation of motion:

$$\mathrm{i}\hbar \frac{\partial}{\partial t} \hat{\mathcal{O}} = [\hat{\mathcal{O}}(t), H + H_I]. \tag{9}$$

Insert the two operator products given in equations (7) and (8) into equation (9). By using the commutation relations of the Fermion operators, employing the screened Hartree–Fock approximation by using a time-dependent static screening [24], and after a lengthy derivation, the final equation of motion can be written as

$$\begin{aligned} \mathrm{i}\hbar \frac{\partial}{\partial t} n_{1,k} = \mathrm{i}\hbar \left.\frac{\partial n_{1,k}}{\partial t}\right|_{\mathrm{Col}} + 2\mathrm{i} \cdot \mathrm{Im}(\mu_{21} E(t) p^*_{21,k}) + 2\mathrm{i} \cdot \mathrm{Im}(\mu_{31} E(t) p^*_{31,k}) \\ - \sum_{k' \neq k} V^{2112}_{|k-k'|} (p_{21,k} p^*_{21,k'} - p^*_{21,k} p_{21,k'}) \\ - \sum_{k' \neq k} V^{3113}_{|k-k'|} (p_{31,k} p^*_{31,k'} - p^*_{31,k} p_{31,k'}) \end{aligned} \tag{10}$$

$$\mathrm{i}\hbar\frac{\partial}{\partial t}n_{2,k} = \mathrm{i}\hbar\frac{\partial n_{2,k}}{\partial t}\bigg|_{\mathrm{Col}} - 2\mathrm{i}\cdot\mathrm{Im}(\mu_{21}E(t)p^*_{21,k}) + 2\mathrm{i}\cdot\mathrm{Im}(\mu_{32}E(t)p^*_{32,k}) + \sum_{k'\neq k} V^{2112}_{|k-k'|}(p_{21,k}p^*_{21,k'} - p^*_{21,k}p_{21,k'}) - \sum_{k'\neq k} V^{3223}_{|k-k'|}(p_{32,k}p^*_{32,k'} - p^*_{32,k}p_{32,k'}) \tag{11}$$

$$\mathrm{i}\hbar\frac{\partial}{\partial t}n_{3,k} = \mathrm{i}\hbar\frac{\partial n_{3,k}}{\partial t}\bigg|_{\mathrm{Col}} - 2\mathrm{i}\cdot\mathrm{Im}(\mu_{31}E(t)p^*_{31,k}) - 2\mathrm{i}\cdot\mathrm{Im}(\mu_{32}E(t)p^*_{32,k}) - \sum_{k'\neq k} V^{3113}_{|k-k'|}(p_{31,k'}p^*_{31,k} - p^*_{31,k'}p_{31,k'}) - \sum_{k'\neq k} V^{3223}_{|k-k'|}(p_{32,k}p^*_{32,k'} - p^*_{32,k}p_{32,k'}) \tag{12}$$

$$\mathrm{i}\hbar\frac{\partial}{\partial t}p_{21,k} = (\varepsilon_{2,k} - \varepsilon_{1,k})p_{21,k} - (\mu_{21}E(t)(n_{1,k} - n_{2,k}) + \mu_{31,k}E(t)p^*_{32,k} + \mu_{32}E(t)p_{31,k}) + \sum_{k'\neq k} V^{1111}_{|k-k'|}n_{1,k'}p_{21,k} - \sum_{k'\neq k} V^{2222}_{|k-k'|}n_{2,k'}p_{21,k} - \sum_{k'\neq k} V^{2112}_{|k-k'|}n_{1,k}p_{21,k'} + \sum_{k'\neq k} V^{2112}_{|k-k'|}n_{2,k}p_{21,k'} + \sum_{k'\neq k} V^{3113}_{|k-k'|}p^*_{32,k}p_{31,k'} - \sum_{k'\neq k} V^{3223}_{|k-k'|}p^*_{32,k'}p_{31,k} + \mathrm{i}\hbar\frac{\partial p_{21,k}}{\partial t}\bigg|_{\mathrm{Col}} \tag{13}$$

$$\mathrm{i}\hbar\frac{\partial}{\partial t}p_{32,k} = (\varepsilon_{3,k} - \varepsilon_{2,k})p_{32,k} - (-\mu^*_{21}E^*(t)p_{31,k} + \mu_{31,k}E(t)p^*_{21,k} + \mu_{32}E(t)(n_{2,k} - n_{3,k})) + \sum_{k'\neq k} V^{2222}_{|k-k'|}n_{2,k'}p_{32,k} - \sum_{k'\neq k} V^{3333}_{|k-k'|}n_{3,k'}p_{32,k} + \sum_{k'\neq k} V^{2112}_{|k-k'|}p_{31,k}p^*_{21,k'} - \sum_{k'\neq k} V^{3113}_{|k-k'|}p^*_{21,k}p_{31,k'} - \sum_{k'\neq k} V^{3223}_{|k-k'|}p_{32,k'}n_{2,k} + \sum_{k'\neq k} V^{3223}_{|k-k'|}p^*_{32,k'}n_{3,k} + \mathrm{i}\hbar\frac{\partial p_{32,k}}{\partial t}\bigg|_{\mathrm{Col}} \tag{14}$$

$$\mathrm{i}\hbar\frac{\partial}{\partial t}p_{31,k} = (\varepsilon_{3,k} - \varepsilon_{1,k})p_{31,k} - (-\mu_{21}E(t)p_{32,k} + \mu_{31,k}E(t)(n_{1,k} - n_{3,k}) + \mu_{32}E(t)p_{21,k}) + \sum_{k'\neq k} V^{1111}_{|k-k'|}n_{1,k'}p_{31,k} - \sum_{k'\neq k} V^{3333}_{|k-k'|}n_{3,k'}p_{31,k} + \sum_{k'\neq k} V^{2112}_{|k-k'|}p_{32,k}p_{21,k'} - \sum_{k'\neq k} V^{3223}_{|k-k'|}p_{21,k}p_{32,k'} - \sum_{k'\neq k} V^{3113}_{|k-k'|}p_{31,k'}n_{1,k'} + \sum_{k'\neq k} V^{3113}_{|k-k'|}p_{31,k'}n_{3,k} + \mathrm{i}\hbar\frac{\partial p_{31,k}}{\partial t}\bigg|_{\mathrm{Col}}. \tag{15}$$

The collision terms $\frac{\partial\hat{\mathcal{O}}}{\partial t}|_{\mathrm{Col}}$ in the above equations describe electron phonon scattering, electron impurity interactions, etc. Taking these effects into any explicit computation involves significant complexity. It is sufficient to treat these incoherent scattering terms by introducing phenomenological decay and dephasing constants to the equations. It is clearly seen from the equations that Coulomb effects can act as the subband energy renormalization and bleaching of the peaks in the absorption spectra [24]. These qualitative effects can be explained at the Hartree–Fock level of our theoretical model. In solving these equations, carrier

conservation is obeyed. These equations can be solved by the fourth order Runge–Kutta method.

As stated in the following section, the far-infrared response is related to the polarization between the upper two subbands (p_{32}). This polarization can oscillate on the frequency around the energy splitting of the two subbands. Before any numerical investigation, it is useful to present an analytical solution to the problem from which we can gain physical insight. First, we assume that each pulse duration is much shorter than the system response times. So the optical fields can be described by impulsive functions:

$$E(t) = E_0\delta(t) + E_0\delta(t - T)\cos(\Delta\psi), \tag{16}$$

where T and $\Delta\psi$ are the delayed time and the shifted phase of the two pulses. Next we assume that the dephasing time is long enough. The dephasing time can be treated as infinite. Finally, another important assumption is that the carrier density is very low. The Coulomb effect can be neglected. This assumption can remove the integral contributions in the semiconductor Bloch equations presented above. Under these conditions, the equation for p_{32} can be simplified as

$$\mathrm{i}\hbar\frac{\partial}{\partial t}p_{32} = \varepsilon_{32}p_{32} + \mu_{21}E(t)p_{31} - \mu_{31}E(t)p_{21}. \tag{17}$$

This is a simple differential equation. Various methods can be applied to solve it. In [14], perturbation expansions are used to obtain an analytical solution. Here we apply a Fourier transform in solving the above equations. After some mathematical calculations, the solution of polarization $p_{32}(t)$ has the following form:

$$\begin{aligned} p_{32}(t) = {} & \frac{E_0}{\hbar}(\mu_{21}p_{31}(0) - \mu_{31}p_{21}(0))\mathrm{e}^{-\mathrm{i}\omega_{32}t}\Theta(t) \\ & + \frac{E_0}{\hbar}(\mu_{21}p_{31}(T) - \mu_{31}p_{21}(T))\cos(\Delta\psi)\mathrm{e}^{-\mathrm{i}\omega_{32}(t-T)}\Theta(t-T), \end{aligned} \tag{18}$$

where $\Theta(t)$ is the Heavyside step function. The solution of p_{32} is relevant to the exact value of p_{31} and p_{21} at the moment T. Since the ultrafast optical field is approximated by a delta function, the time evolution of p_{32} is not coupled to the time dependent functions— $p_{31}(t)$ and $p_{21}(t)$. It is obvious that the time evolution of p_{32} is the interference of two oscillating parts. The oscillating frequency is just the energy splitting of the upper two subbands ($\omega_{32} = E_{32}/\hbar$). Whether it is a constructive interference or a destructive one is determined by the delayed time (T) and the shifted phase ($\Delta\psi$). By carefully adjusting the delayed time and shifted phase, we can get constructive or destructive interference, respectively. In our case, the energy splitting of the upper two subbands is in the THz range. Schemes of coherent control of THz emission by adjusting the delayed time and shifted phase of the two optical pulses are expected. A similar analysis can be made to the time evolution of subband carrier populations and polarizations.

3. Numerical results

The structure of the symmetric quantum well is depicted in figure 1, where a 6.8 nm GaAs deep well layer with an adjacent 18.6 nm $Al_{0.21}Ga_{0.79}As$ step is sandwiched between thick $Al_{0.35}Ga_{0.65}As$ barrier layers. An asymmetric potential is needed to break the parity so that the transition from the ground level to the third subband is permitted. By solving Schrödinger's equation and Poisson's equation self-consistently, the subband eigenenergies and eigenwavefunctions can be obtained as shown in figure 1. The energy separation between the second subband and the third subband $\hbar\omega_{32}$ is about 12 meV, which is in the THz range. THz radiation can be emitted by charge oscillation in these two subbands. The energy separation between the ground subband and the second subband $\hbar\omega_{21}$ is at the midinfrared spectrum of

122 meV. The imposed optical pulse has a central frequency $\hbar\omega_0 = (\hbar\omega_{21} + \hbar\omega_{31})/2$. The pulse electric field is set to be 1×10^6 V m^{-1}. In our simulation, these pulses are set to be Gaussian envelopes with a duration of 100 fs. Such optical sources are available in practice. Sources of intense, approximately 50–150 fs, mid-infrared pulses with a tuning capability from 3 to 20 μm have been reported recently [30]. Pulses of only 120 fs duration are obtained for longer wavelengths ($\lambda > 8$ μm). There are several mechanisms of dephasing, such as electron–electron interaction, electron–phonon scattering, and scattering by impurities. These effects can be considered in our simulation either by adding exact interacting terms (such as the electron interactions in equation (5)) to the total Hamiltonian or by setting phenomenological decay and dephasing constants in the calculations. The Coulomb interactions are directly related to the carrier concentration. In our simulation, the total doping density is set to be 1×10^{11} cm^{-2}, which is not high. The main result of choosing this value is to avoid Coulomb effects on suppression of the THz response. The phenomenological longitudinal lifetimes and the dephasing times corresponding to the other scattering mechanics are set to be a typical value of 1 meV [15, 25]. When the semiconductor nanostructure is illuminated by two identical time delayed and phase shifted pulses, the carrier density in each subband and the intersubband polarization can be obtained by solving the set of equations of motion within a fourth order Runge–Kutta algorithm.

From the discussion above, we can see that the carrier density exhibits an oscillation behaviour as a function of the phase shift between the pulses. The time evolution of subband populations for different time delay and phase shift conditions has been calculated. The numerical results are plotted in figure 2. This shows the relation between the upper two subbands' population evolution and the two pulses' phase delay. Figure 2(a) displays the population of subband 3, and figure 2(b) is the population of subband 2. The beating in the total light field leads to an oscillatory rise in the subband population. The peak value of different subband populations appears at phase delay. Thus the selective population of different subbands can be achieved by adjusting the phase delay conditions. This selective population is displayed in figure 3 at two specific phase conditions, where one of the subband transitions is suppressed. By choosing the phase shift $\Delta\psi = \pi + \omega_{21}\Delta\tau$, the spectrum intensity at ω_{21} will be zero. The electron population in subband 2 by optical pumping from the ground subband will be much less than that in subband 3. In contrast, if the phase shift $\Delta\psi = \pi + \omega_{31}\Delta\tau$, the electron population in subband 3 will be greatly suppressed during the pulse duration. From figure 3, it can be clearly seen that the three subband system can be treated as if one of the upper subbands does not exist by adjusting the time delay and phase shift of these two pulses. This enables us to decouple a selected transition from the neighbouring ones, and, as a result, achieve any prescribed absolute population in the subband. In a semiclassical picture, this selective transition can be interpreted as simultaneously coherent construction and destruction of the carrier densities in different conduction subbands due to pulse interferences. The first pulse generates the carrier densities of each subband, while the second pulse might produce constructive or destructive interference with the first one. Whether the carrier densities in the subband are constructively enhanced or destructively depressed is determined by the phase shift conditions between these pulses.

After excitation with a short laser pulse, THz radiation can be emitted by the charge oscillations in the quantum structure [31]. The large bandwidth of the ultrafast pulses allows the simultaneous phase-coherent excitation of intersubband transitions from the upper two subbands to the lowest ground subband. The coupling of both intersubband transitions via their common state in the ground level generates a quantum coherence between the upper two subbands. This gives rise to quantum beats in the overall polarization oscillating at the difference frequency [32]. Active control of THz radiation evolution by interband

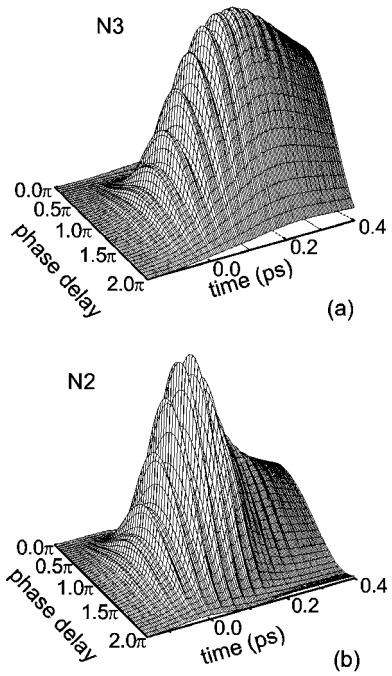

Figure 2. Subband population evolution at different phase delay conditions: (a) represents the population evolution of subband 3 and (b) represents the population evolution of subband 2. Appearances of the maximum value of subband population can be coherently controlled by the phase delay conditions.

coupling phase-locked optical pulses has been theoretically predicted and experimentally demonstrated [14, 15]. THz radiation signal is also obtained in our numerical results under the intersubband coupling schemes discussed above. From electromagnetic theories, the THz radiation electric field is obtained from the second derivative of the induced polarization in the upper two subbands. The time dependent far-infrared polarization can be written as

$$P_{\mathrm{THz}}(t) = 2\sum_{k} \mathrm{Re}(d_{32,k}\, p_{32,k}(t)). \tag{19}$$

From the calculated polarization, the radiated THz electric field can be obtained from $E_{\mathrm{THz}}(t) \propto \partial^2 P_{\mathrm{THz}}(t)/\partial t^2$ [14, 15]. The electric field of the THz signal can be measured by a photoconducting dipole antenna. The origin of the terahertz radiation is that in an electric field, a coherent superposition of the upper two subbands leads to charge oscillations in the well at the subbands' splitting frequency. We can look at the far-infrared generation process as a resonant second-order nonlinear optical frequency conversion process in which light at mid-infrared frequencies within the bandwidth of the laser pulse is mixed to generate the difference frequency in the far-infrared region. In figure 4, the time dependent far-infrared polarization is presented. The far-infrared polarization is sensitive to the time delay and phase shift conditions. Under different selective transition phase conditions, the polarization also has a phase shift and amplitude variation, as can be seen from figure 4. This can be explained as the interference of the two THz pulses induced by the time separated ultrafast coupling laser pulse. Thus the interference of the two pulse excitation can be used not only to control the subband populations, but also to shift the phase of the emitted THz pulses. From the nonlinear optics point of view, the emitted THz signal is a resonant difference-frequency mixing process in the three subbands system. Frequency mixing is induced by the various spectral components of the ultrafast pulse [15, 33]. This method, which can manipulate electronic transitions by the relative phase between two light fields, presents us with a powerful tool for the controlling the operation principles of semiconductor ultrafast optoelectronic devices.

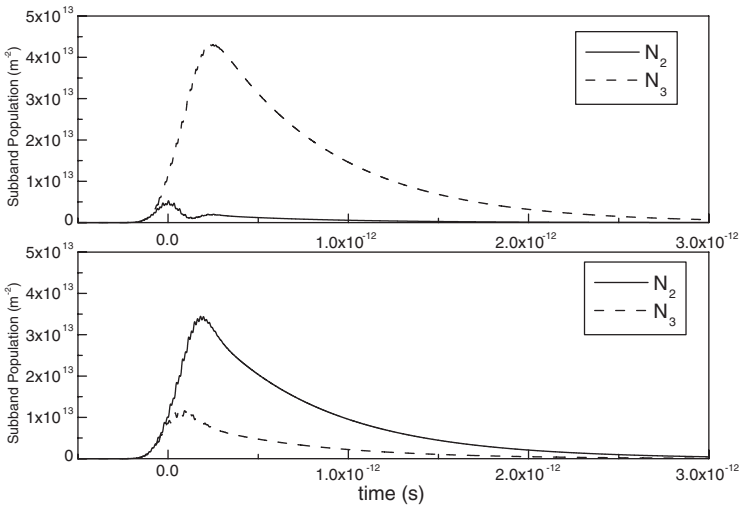

Figure 3. Selective transition in the asymmetric quantum well with different phase shift conditions. The temporal evolution of the upper two subband populations is displayed. The Gaussian pulse has a width of 100 fs, and the time delay between the two pulses is fixed to be 50 fs. The phase shift conditions are $\Delta\psi = \pi + \omega_{21}\Delta\tau$ for the upper panel and $\Delta\psi = \pi + \omega_{31}\Delta\tau$ for the lower panel. As can be seen from the figure, the transition from $|1\rangle$ to $|2\rangle$ is suppressed in the first case and the transition from $|1\rangle$ to $|3\rangle$ is suppressed in the latter case.

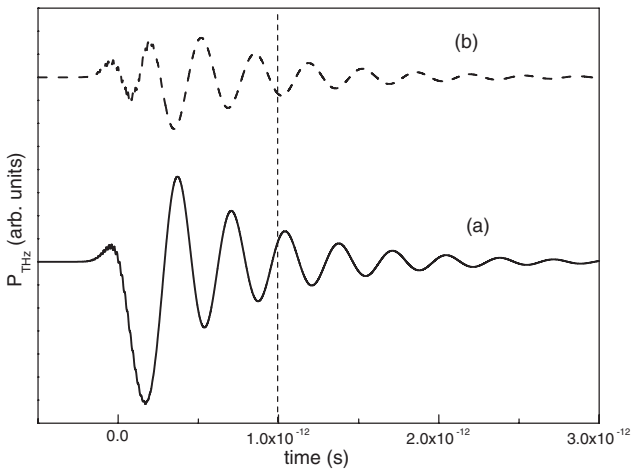

Figure 4. The calculated time dependence of polarization at different selective transition phase conditions. The spectrum intensity at ω_{31} is set to be zero in (a) and the spectrum at ω_{21} is set to be zero in (b). From the vertical dashed line, the phase shift can be identified.

4. Conclusions

In conclusion, we have demonstrated that it is feasible to control the subband populations and carrier oscillation in the subbands of a semiconductor nanostructure by two-pulse excitation. Under different time delay and phase shift conditions the subband population can be selectively excited. A controllable subband population filling by optical pumping is realized. These optical excitation can lead to THz radiation from the asymmetric quantum wells. The phase and amplitude of THz radiation is found to be sensitive to the optical interference of the coupling

pulses. In our simulation, Coulomb effects under the screened Hartree–Fock approximation are taken into account. In our results, the THz response is found to be greatly influenced by Coulomb interactions. When the carrier density is high, electron–electron interactions can be essential, and these suppress the THz response. Coulomb effects can be avoided by keeping the concentrations in the sample low enough. These results will be useful for THz sources produced by optically pumping semiconductor quantum well structures.

Acknowledgments

We would like to acknowledge Dr Z P Jian and Dr B C Guo for helpful discussions. This work was supported by the National Natural Science Foundation of China (10390162), the Special Funds for Major State Basic Research Project (2001CCA02800G and 20000683), and the Funds from the Shanghai Municipal Commissions of Science and Technology of China (011661075, 03JC14082).

References

[1] Rabitz H, de Vivie-Riedle R, Motzkus M and Kompa K 2000 *Science* **288** 824
[2] Wei C J, Suter D, Windsor A S M and Manson N B 1998 *Phys. Rev.* A **58** 2310
[3] Bergmann K, Theuer H and Shore B W 1998 *Rev. Mod. Phys.* **70** 1003
[4] Netz R, Nazarkin A and Sauerbrey R 2003 *Phys. Rev. Lett.* **90** 063001
[5] Elsaesser T and Woerner M 1999 *Phys. Rep.* **321** 253
[6] McPeake D, Vasko F T and O'Reilly E P 2003 *Phys. Rev.* B **68** 193306
[7] Cao J C 2003 *Phys. Rev. Lett.* **91** 237401
[8] Khurgin J B and Rosencher E 1996 *IEEE J. Quantum Electron.* **32** 1882
[9] Mompart J, Corbalan R and Roso L 2002 *Phys. Rev. Lett.* **88** 023603
[10] Rossi F and Kuhn T 2002 *Rev. Mod. Phys.* **74** 895
[11] Pötz W 1997 *Phys. Rev. Lett.* **79** 3262
[12] Sadeghi S M, van Driel H M and Fraser J M 2000 *Phys. Rev.* B **62** 15386
[13] Planken P C M, Nuss M C, Brener I, Goossen K W, Luo M S C, Chuang S L and Pfeiffer L 1992 *Phys. Rev. Lett.* **69** 3800
[14] Luo M S C, Chuang S L, Planken P C M, Brener I and Nuss M C 1993 *Phys. Rev.* B **48** 11043
[15] Planken P C M, Brener I, Nuss M C, Luo M S C and Chuang S L 1993 *Phys. Rev.* B **48** 4903
[16] Feldmann J, Leo K, Shah J, Miller D A B, Cunningham J E, Meier T, von Plessen G, Schulze A, Thomas P and Schmitt-Rink S 1992 *Phys. Rev.* B **46** 7252
[17] Leo K 1998 *Semicond. Sci. Technol.* **13** 249
[18] Cao J C, Liu H C and Lei X L 2000 *J. Appl. Phys.* **87** 2867
[19] Heberle A P, Baumberg J J and Köhler K 1995 *Phys. Rev. Lett.* **75** 2598
[20] Heberle A P, Baumberg J J, Binder E, Kuhn T, Köhler K and Ploog K H 1996 *IEEE J. Sel. Top. Quantum Electron.* **2** 769
[21] Liu H C and Capasso F (ed) 2000 *Intersubband Transition in Quantum Wells Physics and Device Applications II* (*Semiconductors and Semimetals* vol 66) (San Diego, CA: Academic)
[22] Liu H C, Cheung I W, SpringThorpe A J, Dharma-wardana C, Wasilewski Z R, Lockwood D J and Aers G C 2001 *Appl. Phys. Lett.* **78** 3580
[23] Wu B H, Cao J C, Xia G Q and Liu H C 2003 *Eur. Phys. J.* B **33** 9
[24] Haug H and Koch S W 1994 *Quantum Theory of the Optical Properties of Semiconductors* 3rd edn (Singapore: World Scientific)
[25] Nikonov D E, Imamoğlu A, Butov L V and Schmidt H 1997 *Phys. Rev. Lett.* **79** 4633
[26] Chansungsan C, Tsang L and Chuang S L 1994 *J. Opt. Soc. Am.* B **11** 250
[27] Nikonov D E, Imamoğlu A and Scully M O 1999 *Phys. Rev.* B **59** 12212
[28] Batista A A, Tamborenea P I, Birnir B, Sherwin M S and Citrin D S 2002 *Phys. Rev.* B **66** 195325
[29] Pötz W 1998 *Appl. Phys. Lett.* **72** 3002
[30] Kaindl R A, Wurm M, Reimann K, Hamm P, Weiner A M and Woerner M 2000 *J. Opt. Soc. Am.* B **17** 2086
[31] Meier T, von Plessen G, Thomas P and Koch S W 1995 *Phys. Rev.* B **51** 14490
[32] Joschko M, Woerner M, Elsaesser T, Binder E, Kuhn T, Hey R, Kostial H and Ploog K H 1997 *Phys. Status Solidi* b **204** 23
[33] Shen Y R 1984 *The Principles of Nonlinear Optics* (New York: Wiley)